RSC Advances

PAPER

View Article Online
View Journal | View Issue

Cite this: *RSC Adv.*, 2021, **11**, 30222

Pyrene-based ammonium bromides combined with g-C_3N_4 for the synergistically enhanced fixation reaction of CO_2 and epoxides†

Tao Chang,[ab] Xiaopeng Li,[a] Yongjing Hao,[a] Lianwei Kang,[a] Tian Tian,*[a] Xiying Fu,[a] Zheng Zhu,*[a] Balaji Panchal[a] and Shenjun Qin*[a]

Received 11th July 2021
Accepted 26th August 2021

DOI: 10.1039/d1ra05328k

rsc.li/rsc-advances

A new type of pyrene-based ammonium bromides (PABs) was synthesized *via* the reaction of bromomethyl pyrene and tertiary amines with different alkyl chains combined with graphitic carbon nitride (g-C_3N_4) through π–π stacking interactions. The new pyrene-based ammonium bromides were investigated both in homogenous phase and heterogeneous phase combining with g-C_3N_4 for the CO_2 fixation reaction of epoxides under mild conditions. Obviously, the combination was proved to be an efficient system for the conversion of epoxides. The interaction between g-C_3N_4 and PABs was confirmed by quantum chemical calculations. g-C_3N_4/Py-C_{12} exhibited an excellent yield of cyclic carbonates (above 93%) at 80 °C, atmospheric pressure and solvent-free conditions. A preliminary kinetic study was performed using g-C_3N_4/Py-C_{12} and the activation energy was calculated to be 61.5 kJ mol^{-1}.

Introduction

The anthropogenic carbon dioxide emission in atmosphere has far-reaching effects on sustainable society, and is considered as a major component of global greenhouse gas, leading to global warming and extreme weather events.[1] However, the effective conversion of CO_2 into high value-added chemicals has attracting widespread attention to scientists, because of which it has been regarded as an alternative, nontoxic, and sustainable C1 resource.[2–7] Among these conversions, the generation of cyclic carbonates, a popular group of chemicals, is recognized as an effective route to convert inert CO_2 with epoxides.[8–16] In addition, cyclic carbonates are established as not only valuable materials with various industrial applications for polymer synthesis, aprotic polar solvents, fuel additives and electrolyte solvents in lithium-ion batteries but also crucial intermediates in the manufacturing of fine chemicals.[17,18]

In fact, there are quite a few materials on the utilization of CO_2 fixation, including homogeneous and heterogenous catalysts, for example, ionic liquids,[19,20] organocatalysts,[21–23] Salen,[24–26] porphyrins,[27] alkali salts,[28] covalent-organic frameworks (COFs),[29] metal–organic frameworks (MOFs)[30] and covalent organic polymers (COPs).[9,31] More intriguingly, some quaternary ammonium salts have been selected as catalysts for CO_2 fixation with epoxides, which are more sustainable than traditional Lewis acid (base) alternatives because of such suit of metal-free organocatalysts according to a green chemistry view point.[32–37] Apparently, with regard to ammonium catalysts, hydrogen bonding activating strategy of epoxides is crucial for accomplishing CO_2 fixation.[38] In addition, the conversion of CO_2 to cyclic carbonates under mild conditions, such as low reaction temperature, atmospheric pressure, metal-free and solvent-free, is still challenging.

Recently, the syntheses and application of 2D materials of graphite carbon nitride (g-C_3N_4) have attracted wide attention on CO_2 absorption due to the large amount of basic groups of amine and guanidine as nucleophilic sites for CO_2 activation.[39] It is predicted that the as-prepared and adjusted g-C_3N_4 could be optimized as catalysts for the capture and conversion of CO_2.[40–54] The C_3N_4 materials could be selected independently as the catalysts for CO_2 fixation with epoxides; however, these processes suffer from severe reaction conditions to obtain excellent conversion.[41,46,56] Some strategies were developed to increase the activity of C_3N_4 materials, including adjusted acid-base duality with doping of metal atoms,[40,49,54] alkalis,[43] phosphorous,[44] metal halides,[45] and boric acid.[50,51] Another is that co-catalysts, such as tetrabutyl ammonium bromide (TBAB),[44,48,54] KI,[50] and DMF,[53] are introduced and combined with g-C_3N_4, which play a crucial role in accelerating the rate-limiting step of opening epoxides by the nucleophilicity of halide anions.[28,31] Although significant advances have been accomplished in g-C_3N_4 syntheses, some protocols suffer from harsh conditions, such as high temperature, high pressure and

[a]*Key Laboratory of CO_2 Utilization of Handan City, College of Material Science and Engineering, Hebei University of Engineering, Handan 056038, Hebei, China. E-mail: tiantian19860102@126.com; zhuzheng@hebeu.edu.cn; sjqin528@hebeu.edu.cn*

[b]*Key Laboratory of Heterocyclic Compounds of Hebei Province, Handan College, Handan 056005, Hebei, China*

† Electronic supplementary information (ESI) available. See DOI: 10.1039/d1ra05328k

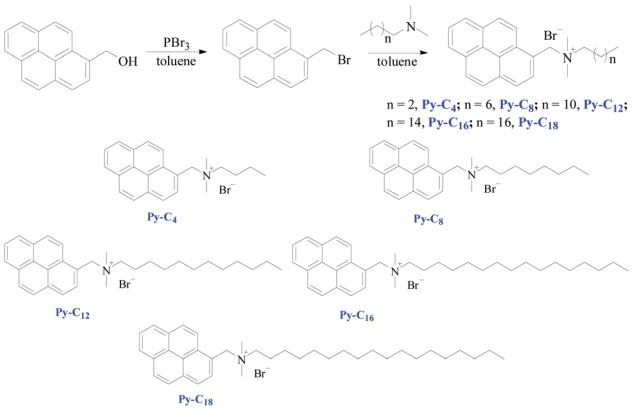

Scheme 1 General synthesis strategy of pyrene-based quaternary ammonium salts.

the presence of metal salts and co-solvents. In addition, most of the optimized procedures focus on modulating the texture structure and surface properties of g-C_3N_4. Predictably, the development of novel catalysts is still a fascinated alternative, which could interact tightly and realize the reaction synergistically with g-C_3N_4.

In contrast, the non-covalent methodology is more convenient and effective for the catalyst construction without the chemical modification of homogeneous catalysts.[55] The π–π stacking interactions are an available non-covalent immobilization, and g-C_3N_4 provides a significant alternative for non-covalent adjustment *via* π–π stacking interactions with polyaromatic molecules, such pyrene-based moiety.[56] From the above point, the preparation of a pyrene-based non-covalent catalyst anchored on the g-C_3N_4 surface is a potentially valuable strategy of the heterogenization of homogeneous catalysis. Herein, quaternary ammonium salts connected with pyrene-based tag and different substituted alkyl chains, which possessed the properties of immobilization onto the g-C_3N_4 surface, are accordingly reported (Scheme 1).

Results and discussion

In order to illustrate the potentiality for a catalytic reaction, the fixation of epichlorohydrin and CO_2 as a model reaction was

Table 1 Effect of the structure of Py-C_n[a]

Entry	Catalysts	Yield (%)
1	Py-C_4	46.4
2	Py-C_8	50.9
3	Py-C_{12}	53.8
4	Py-C_{16}	53.6
5	Py-C_{18}	51.3
6[b]	DTAB	30.5

[a] Reaction conditions: ECH (10 mmol, 0.78 mL), catalysts (0.0375 mmol), CO_2 (0.1 MPa), 70 °C, 8 h. [b] DTAB: dodecyl trimethyl ammonium bromide.

Table 2 Effect of the combined catalysts of Py-C_n and g-C_3N_4[a]

Entry	Py-C_n/C_3N_4	Yield (%)
1	Py-C_4/g-C_3N_4	62.5
2	Py-C_8/g-C_3N_4	65.7
3	Py-C_{12}/g-C_3N_4	75.2
4	Py-C_{16}/g-C_3N_4	72.7
5	Py-C_{18}/g-C_3N_4	72.0
6	DTAB/g-C_3N_4	42.6
7[b]	g-C_3N_4	NR

[a] Reaction conditions: ECH (10 mmol, 0.78 mL), Py-C_n (0.0375 mmol), g-C_3N_4 (12 mg), CO_2 (0.1 MPa), 70 °C, 8 h. [b] In the absence of Py-C_n, no reaction.

implemented in the presence of pyrene-based ionic liquids under mild conditions (Table 1, entries 1–5). Gratifyingly, all ionic liquids fabricated with mediated alkyl chains exhibited considered activities, which were superior to that of dodecyl trimethyl ammonium bromide (entry 6). Therefore, it is of significance to explore such catalysts deeply. As shown in Tables 1 and 2, when Py-C_n was used with different substitutes, there was only a slight change. The trend is that with the increase in the length of alkyl chains, the carbonate yield was ascending marginally. Predictably, the combination of g-C_3N_4 and Py-C_n was selected as the catalyst for CO_2 conversion because a large number of amine and guanidine groups were grafted, which are beneficial to the absorption and activation of CO_2. An increase in the fixation of CO_2 was detected in the presence of g-C_3N_4 (Table 2, entries 1–5). Thus, it is certain that g-C_3N_4 plays a crucial role in realizing the CO_2 fixation reaction. The results were better than that of DTAB combined with Py-C_n, which meant that Py-C_n could interact with g-C_3N_4. Therefore, a synergistic effect through π–π stacking interactions between Py-C_n and g-C_3N_4 was proposed, which is significant to realize the organic reaction.[57,58]

The reaction time was found to influence the CO_2 fixation and be an important factor to realize the reaction completely. Then, the influence of the reaction time ranged from 4 to 24 h on the CO_2 conversion was explored. As demonstrated in Fig. 1, the cyclic carbonates yield increased with prolonged time, and

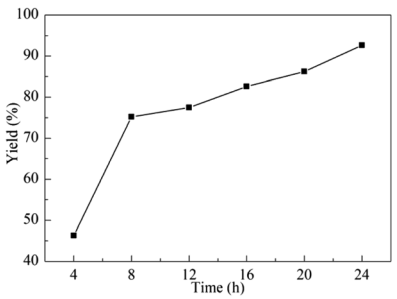

Fig. 1 Effect of the reaction time. Reaction conditions: ECH (10 mmol, 0.78 mL), g-C_3N_4 (12 mg), Py-C_{12} (0.0375 mmol, 19 mg), CO_2 (0.1 MPa), 70 °C.

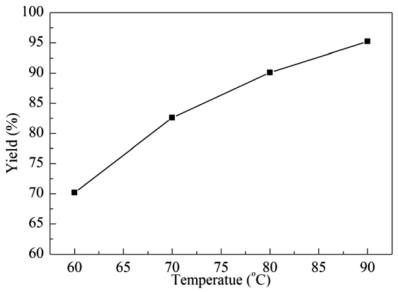

Fig. 2 Effect of the reaction temperature. Reaction conditions: ECH (10 mmol, 0.78 mL), g-C_3N_4 (12 mg), Py-C_{12} (0.0375 mmol, 19 mg), CO_2 (0.1 MPa), 16 h.

75.2% yield was obtained after 8 h. From 8 h to 24 h, the well-distributed growth trend of the yield was detected. Therefore, the appropriate reaction time was selected as 16 h, beneficially, this time was not only effective, but also more economical.

Temperature plays a crucial effect on organic reactions. Thus, the influence of temperature varied from 60 °C to 90 °C was investigated for the fixation reaction of ECH with CO_2. As shown in Fig. 2, the yield improved rapidly when the reaction was carried out at 60 °C after 16 h, and a yield of 70.2% was detected. The varied yields of 82.6%, 90.1% and 95.2% were obtained when the temperature was risen from 70 °C to 90 °C. Although an excellent yield was explored at 90 °C, temperature of 80 °C was reasonable according to the energy cost.

The yield is strongly related to the amount of the combined catalyst in this reaction. The results were illustrated in Table 3. A yield of 80.1% was obtained at a low catalyst amount with a constant ratio of g-C_3N_4 to Py-C_{12} (entry 1) because lower catalytic concentration can not provide sufficient active sites to promote the reaction availably. Increasing the catalyst amount improved the activity of this combined system because of the enhancing synergistic interaction between the catalyst and substrates. A superior yield of 95.2% was observed, and a substantial increase was not obtained by increasing the catalytic amount to higher than 15 mg and 23.8 mg of g-C_3N_4 and Py-C_{12}, respectively.

In order to expand the versatility of the present catalytic system, the catalyst of Py-C_{12} with g-C_3N_4 was evaluated for the CO_2 fixation of various epoxides at optimum reaction conditions. All results are summarized in Table 4; as expected, excellent yields varied from 93% to 96% were observed for all epoxides tethered with diverse functional groups. Epoxides exhibited different conversion ability, and some epoxides such as ECH, epibromohydrin, glycidyl phenyl ether and allyl glycidyl ether were converted within 16 h (entries 1–4). In contrast, butyl glycidyl ether and styrene oxide needed a slightly longer time to obtain high yields (entries 5 and 6). In addition, glycol diglycidyl ether could also be considered as a candidate substrate and generated into corresponding cyclic carbonate with good yield at 48 h (entry 7).

Table 3 Effect of the catalyst amount[a]

Entry	g-C_3N_4 (mg)	Py-C_{12} (mg)	Yield (%)
1	9	14.3	80.1
2	12	19	82.6
3	15	23.8	95.2
4	18	28.5	96.0

[a] Reaction conditions: ECH (10 mmol, 0.78 mL), CO_2 (0.1 MPa), 80 °C, 16 h.

Table 4 Synthesis of cyclic carbonates catalyzed by Py-C_{12} in the presence of g-C_3N_4[a]

Entry	Epoxides	Product	Yield[b] (%)
1	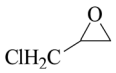	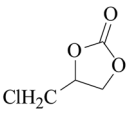	95.2
2	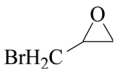	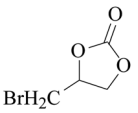	95.8
3	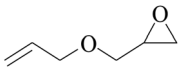	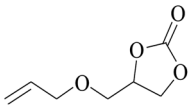	94.9
4	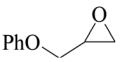	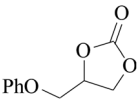	94.8
5[c]	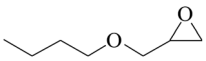	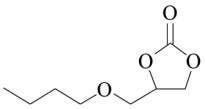	96.5
6[c]		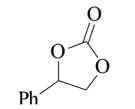	93.5
7[d]	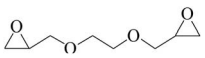	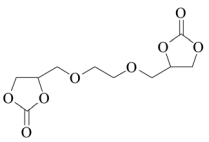	94.6

[a] Reaction conditions: epoxides (10 mmol), g-C_3N_4 (15 mg), Py-C_{12} (23.8 mg), CO_2 (0.1 MPa), 80 °C, 16 h. [b] Detected by ^{1}H-NMR. [c] 32 h. [d] 48 h.

The catalytic activity of g-C_3N_4/Py-C_{12} was compared with other catalysts for the CO_2 fixation reaction, as summarized in Table 5. In most studies, the CO_2 fixation reactions were realized at high temperatures and pressures. Comparatively, the reactions were carried out at mild conditions and with lower catalyst amount in our study.

Clearly, the catalyst could catalyze the fixation reaction of CO_2 by decreasing the activation energy (E_a), along with a high-speed reaction rate at a lower activation energy. In this regard, the capability of Py-C_{12} coordinated with g-C_3N_4 in lowering the activation energy of the fixation reaction was exactly examined at varied temperatures from 50 to 80 °C under the optimum conditions.

Table 5 Comparison of catalytic activity for CO_2 fixation with ECH to the selected reported references

Catalysts	Catalyst amount	Co-catalyst	Reaction conditions	Yield (%)	Reference
Zn-g-C_3N_4/SBA	100 mg	—	150 °C, 3.5 MPa, 1.5 h	99	40
u-g-C_3N_4	100 mg	—	130 °C, 2 MPa, 24 h	99	41
$ZnCl_2$/mp-C_3N_4	200 mg	—	140 °C, 2.5 MPa, 6 h	73	42
g-C_3N_4-500-NaOH	400 mg	—	140 °C, 2 MPa, 6 h	92	43
P-g-C_3N_4	150 mg	TBAB	100 °C, 2 MPa, 3 h	91	44
n-butlBr	200 mg	—	140 °C, 2.5 MPa, 6 h	88	45
u-g-C_3N_4	50 mg	—	130 °C, 3.5 MPa, 2 h	99	46
g-C_3N_4	50 mg	TBAB	105 °C, 1 bar, 20 h	>99	48
Co@N_xC	50 mg	TBAB, CH_3CN	60 °C, 1 bar, 12 h	84	49
BGCN05	100 mg	KI	60 °C, 1 bar, 60 h	73	50
BCN	30 mg	—	130 °C, 3.0 MPa, 24 h	97	51
u-C_3N_4	230 mg	—	120 °C, 2.0 MPa, 2 h	96	52
GO	2.5 mg	DMF	100 °C, 1 bar, 12 h	95	53
2.0Zn@g-C_3N_4-550	50 mg	TBAB	90 °C, 1.5 MPa, 3 h	99	54
g-C_3N_4	15 mg	Py-C_{12}	80 °C, 1 bar, 16 h	95	This work

In general, the rate equation for the CO_2 fixation was represented as eqn (1). Usually, eqn (1) could be simplified as eqn (2), because the reaction was implemented at constant catalyst concentration and excessively CO_2 conditions. According to previous reports, the fixation reaction was described as pseudo first order reaction on the ECH concentration.[59–62] Then, the equation was supported as eqn (3) and (4), where k is the rate constant, t is the reaction time and x is the conversion yield.

$$r = \mathrm{d}x/\mathrm{d}t = k''[\mathrm{ECH}]^{\alpha}[\mathrm{CO_2}]^{\beta}[\mathrm{cat.}]^{\gamma} \quad (1)$$

$$r = \mathrm{d}x/\mathrm{d}t = k'[\mathrm{ECH}]^{\alpha} \quad (2)$$

$$r = \mathrm{d}x/\mathrm{d}t = k'[\mathrm{ECH}] \quad (3)$$

$$\ln(1 - x) = kt + C \quad (4)$$

$$\ln k = E_a/RT + C \quad (5)$$

Therefore, the process kinetics and E_a of the production were investigated, and the results are demonstrated in Tables S1–S5†, Fig. 3 and 4. As shown in Fig. 3, a linear relationship between $\ln(1 - x)$ *versus* time was obtained, that meant that the hypothesis of pseudo first order reaction on the ECH concentration was rational. Thus, the k values described in Table S5† were calculated from curve of $\ln(1 - x)$ *versus* t at various temperatures. The E_a to cyclic carbonates could be obtained according to Arrhenius law (eqn (5)). The slope of lnk *versus* $1/T$ is the value of E_a/T, consequently, the E_a was calculated as 61.5 kJ mol^{-1} (Fig. 4).

In order to investigate the fixation reaction mechanism of CO_2 and epoxides enhanced by pyrene-based ammonium bromides combined with g-C_3N_4, density functional theory (DFT) calculations were performed using a DMol^3 module of Material Studio 2016. Molecular orbitals were used to investigate the type of bonding and the interactions between the new pyrene-based ammonium bromides and g-C_3N_4 during the catalytic process.[63,64] The surfaces of the molecular orbitals were drawn at the 0.03 a. u. iso level, and they described the electron density in both the GS and the excited state in Fig. S1.† In case of g-C_3N_4/Py-C_4 and g-C_3N_4/Py-C_{18}, it was a π-type bond and the electron density was localized on g-C_3N_4 and the tertiary amine group (–$(CH_2)_2$–N–$(CH_3)_2$–) and Br^-. The molecular orbitals that characterized this π-type bond were HOMO orbitals. The process included a slight delocalization of electron density from the g-C_3N_4 ring. On the basis of g-C_3N_4/Py-C_8 and g-C_3N_4/Py-C_{16}, the π-type bond exited between them, and the electron density was localized on the g-C_3N_4 and the pyrenephenyl group. The molecular orbitals that characterized this π-type bond were also HOMO orbitals. The π-extended electron density conjugation appeared as an effect of an intramolecular interaction between

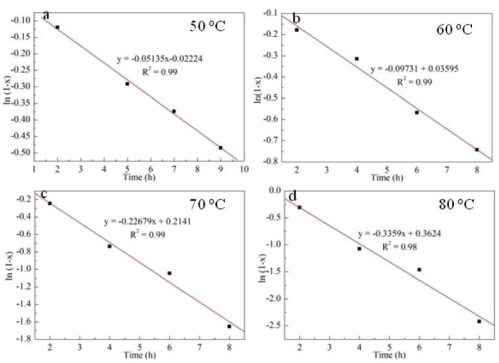

Fig. 3 Logarithmic plots of $(1 - x)$ *versus* time by Py-C_{12} in the presence of g-C_3N_4.

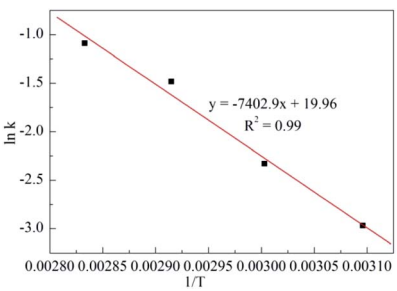

Fig. 4 Arrhenius plots for CO_2 fixation with ECH using Py-C_{12} in the presence of g-C_3N_4.

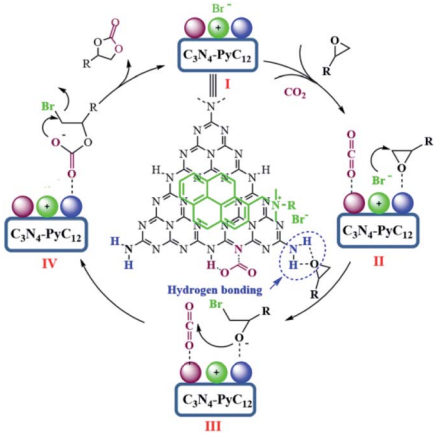

Scheme 2 Probable mechanism for the fixation of CO_2 to epoxides.

pyrenephenyl group and g-C_3N_4 ring. Based on g-C_3N_4/Py-C_{12}, the stronger interaction was π–π conjugation effects, and the electron density was localized on the g-C_3N_4 and the tertiary amine group (–$(CH_2)_2$–N–$(CH_3)_2$–) and Br^-. Meanwhile, the weaker interaction was π → π conjugation effects, and the electron density was localized on the g-C_3N_4 and pyrenephenyl group. Therefore, a series of varying alkyl chain-substituted pyrene-based ammonium bromides combining with g-C_3N_4 by π–π stacking interactions were exhibited to have predominant activity for CO_2 fixation with various epoxides.

Therefore, based on the present experimental and previous references,[31,41,44,50–52] the proposed mechanism derived from the concept of synergetic effect for CO_2 fixation catalyzed by g-C_3N_4/Py-C_{12} is depicted in Scheme 2. First, the interaction of g-C_3N_4 with Py-C_{12} happens through π–π stacking certified by DFT and previous reports.[57,58] Thus, the combined catalytic system is favorable for synergistic inteaction between catalytic sites of amino groups and the nucleophilic reagent (Scheme 2, intermediate **I**). Second, the amino groups in g-C_3N_4 play a significant role in activating the epoxides and carbon dioxide through hydrogen bonding. The activation of epoxides through hydrogen bonding with primary amino group and CO_2 *via* secondary and tertiary amine possibly occurs simultaneously, which allows the coordination of intermediate **II**.[26,41,44] As a result, the increasing electrophilicity of the terminal carbon of epoxides is attacked by the nucleophilic bromide ion from the pyrene-based ammonium interacting tightly with g-C_3N_4 to generate the negative bromo-alkoxide intermediate **III**, which is stabilized by hydrogen bonding. Consequently, the attack of activated CO_2 with bromo-alkoxide and intermediate **IV** of linear bromo-carbonate are generated. Finally, the intramolecular ring-closing of intermediate **IV** occurs, and the generated cyclic carbonate regenerates the catalyst.

Experimental section

Preparation of pyrene based quaternary ammonium salts and g-C_3N_4

Synthesis of bromomethyl pyrene (PyBr). It was synthesized through the reaction of pyrene methanol with PBr_3 under argon gas atmosphere. The classic procedure was as follows: 1-pyrene methanol (1 g, 4.3 mmol) was added into a Schlenk flask, sealed with a rubber tap, and charged with Ar three times. Then, 50 mL anhydrous toluene was injected into the flask, which was placed into an ice bath. PBr_3 (1 mL, 10.5 mmol) was injected into the flask. The mixture was stirred for another 5 h. When the reaction finished, a saturated sodium carbonate solution (20 mL) was added into the flask, the organic phase was separated and washed with 20 mL water and saturated NaCl solution twice, respectively, and dried with anhydrous $MgSO_4$. Finally, most toluene was evaporated and crystalized in a refrigerator. The pale-yellow crystal was obtained, and the yield was 85%.

Synthesis of pyrene based quaternary ammonium salts. Various alkyl-substituted pyrene-based quaternary ammonium salts were prepared *via* the reaction of PyBr with alkyl tertiary amines. PyBr (1.0 g, 3.39 mmol), alkyl tertiary amine (3.39 mmol) and 20 mL toluene were mixed in a flask at 55 °C for 48 h. After the reaction completion, the white solid was filtered, and dried under vacuum.

Py-C_4: ^{1}H NMR (400 MHz, CD_3OD) δ 8.82 (d, J = 9.2 Hz, 1H, ArH), 8.16–8.46 (m, 8H, ArH), 5.39 (s, 2H, $ArCH_2N$), 3.54–3.58 (m, 2H, NCH_2), 3.09 (s, 6H, NCH_3), 1.84–1.88 (m, 2H, NCH_2CH_2), 1.32–1.37 (m, 2H CH_2), 0.97 (t, J = 7.6 Hz, 3H, CH_3); ^{13}C NMR (100 MHz, CD_3OD) δ 132.86. 132.81, 132.16, 131.11, 130.38, 129.38, 129.35, 127.71, 127.21, 126.79, 126.47, 125.23, 124.64, 124.03, 123.96, 122.09, 64.30, 63.92, 49.51, 24.40, 19.87, 14.02; ESI-MS: calcd for $C_{23}H_{26}NBr$, m/z $[M - Br]^+$: 316.2, found: 316.1.

Py-C_8: ^{1}H NMR (400 MHz, CD_3OD) δ 8.80 (d, J = 9.2 Hz, 1H, ArH), 8.16–8.46 (m, 8H, ArH), 5.38 (s, 2H, $ArCH_2N$), 3.5–3.55 (m, 2H, NCH_2), 3.08 (s, 6H, NCH_3), 1.84 (s, 2H, NCH_2CH_2), 1.24–1.30 (m, 10H CH_2), 0.85 (t, 3H, CH_3); ^{13}C NMR (100 MHz, CD_3OD) δ 132.86. 132.77, 132.16, 131.12, 130.39, 129.39, 129.36, 127.71, 127.22, 126.80, 126.47, 125.23, 124.64, 124.03, 123.93, 122.11, 64.47, 63.98, 49.54, 31.61, 28.91, 28.88, 26.41, 22.49, 22.42, 14.42; ESI-MS: calcd for $C_{27}H_{34}NBr$, m/z $[M - Br]^+$: 372.3, found: 372.2.

Py-C_{12}: ^{1}H NMR (400 MHz, $CDCl_3$) δ 8.79 (d, J = 9.32 Hz, 1H, ArH), 8.26 (d, J = 7.88 Hz, 1H, ArH), 7.98–8.08 (m, 3H, ArH), 7.78–7.91 (m, 3H, ArH), 7.64 (d, J = 8.84 Hz, 1H, ArH), 6.04 (s, 2H, $ArCH_2N$), 3.78 (t, J = 7.64 Hz, 2H, NCH_2), 3.30 (s, 6H, NCH_3), 1.71 (s, 2H, NCH_2CH_2), 0.97–1.24 (m, 18H, CH_2), 0.85 (t, J = 6.8 Hz, 3H, CH_3); ^{13}C NMR (100 MHz, $CDCl_3$) δ 132.50, 132.33, 131.85, 130.61, 129.96, 129.54, 128.78, 126.59, 126.20, 126.00, 125.83, 124.24, 123.63, 123.47, 120.07, 65.20, 64.19, 49.36, 31.86, 29.49, 29.45, 29.32, 29.28, 29.25, 26.33, 23.10, 22.68, 14.16; ESI-MS: calcd for $C_{31}H_{42}NBr$, m/z $[M - Br]^+$: 428.3, found: 428.2.

Py-C_{16}: ^{1}H NMR (400 MHz, $CDCl_3$) δ 8.80 (d, J = 9.28 Hz, 1H, ArH), 8.27 (d, J = 7.88 Hz, 1H, ArH), 7.99–8.09 (m, 3H, ArH), 7.79–7.92 (m, 3H, ArH), 7.65 (d, J = 8.84 Hz, 1H, ArH), 6.06 (s, 2H, $ArCH_2N$), 3.79 (t, J = 7.56 Hz, 2H, NCH_2), 3.31 (s, 6H, NCH_3), 1.72 (s, 2H, NCH_2CH_2), 0.97–1.24 (m, 26H, CH_2), 0.87 (t, J = 6.5 Hz, 3H, CH_3); ^{13}C NMR (100 MHz, $CDCl_3$) δ 132.51, 132.34, 131.87, 130.62, 129.98, 129.57, 128.79, 126.59, 126.20, 126.01, 125.84, 124.25, 123.64, 123.48, 120.06, 65.22, 64.20, 49.37, 31.94, 29.72, 29.68, 29.65, 29.57, 29.48, 29.39, 29.35, 29.26,

26.33, 23.11, 22.71, 14.17; ESI-MS: calcd for $C_{35}H_{50}NBr$, m/z $[M - Br]^+$: 484.4, found: 484.3.

Py-C_{18}: ^{1}H NMR (400 MHz, $CDCl_3$) δ 8.77 (d, $J = 8.92$ Hz, 1H, ArH), 8.24 (d, $J = 7.4$ Hz, 1H, ArH), 7.93–8.03 (m, 3H, ArH), 7.76–7.86 (m, 3H, ArH), 7.61 (d, $J = 8.56$ Hz, 1H, ArH), 7.10–7.19 (m, 3H), 5.98 (s, 2H, $ArCH_2N$), 3.77 (s, 2H, NCH_2), 3.25 (s, 6H, NCH_3), 2.29 (s, 2H, NCH_2CH_2), 1.68 (s, 2H, NCH_2CH_2), 0.84–1.21 (m, 30H, CH_2); ^{13}C NMR (100 MHz, $CDCl_3$) δ 137.80, 132.48, 132.30, 131.83, 130.59, 129.93, 129.46, 128.99, 128.75, 128.18, 126.61, 126.17, 125.98, 125.81, 125.26, 124.23, 123.62, 123.49, 120.15, 65.09, 64.19, 49.32, 31.92, 29.70, 29.67, 29.64, 29.56, 29.48, 29.37, 29.29, 29.24, 26.35, 23.10, 22.70, 21.44, 14.16; ESI-MS: calcd for $C_{37}H_{54}NBr$, m/z $[M - Br]^+$: 512.4, found: 512.4.

Synthesis of g-C_3N_4. g-C_3N_4 was synthesized according to a previous study,[65] and in a typical procedure, melamine (20 g) was placed into a quartz boat and heated at 550 °C under N_2 atmosphere for 4 h. The yellow powder was obtained and used without further purification.

Procedure of CO_2 fixation with epoxides

At room temperature, Py-C_n, g-C_3N_4 and epoxides were charged into a Schlenk tube, respectively. To enable the catalysts interact completely, the mixture was sonicated for 20 min. Then, CO_2 was injected into the tube through a balloon, which was placed into a heater and stirred at a fixed temperature. After the reaction, the mixture was cooled at room temperature, and the excess CO_2 was vented. After centrifugation, a small amount of clearly crude product was separated and detected by ^{1}H NMR to identify the conversion.

DFT calculations

The DFT calculations were performed using a DMol^3 module of Material Studio 2016. During optimization, all atoms of the paddlewheel cluster and adsorbing molecules, except terminating atoms, could relax. The generalized gradient approximation (GGA) method with the Perdew–Burke–Ernzerhof (PBE) function was employed to describe the interactions between the core and electrons. An energy cutoff of 450 eV was used for the plane wave expansion of the electronic wave function. The force and energy convergence criteria were set to 0.03 eV Å^{-1} and 10^{-5} eV, respectively.

Conclusions

A series of ranged alkyl chain-substituted pyrene-based ammonium bromides combining with g-C_3N_4 by π–π stacking interactions exhibited a predominant activity towards CO_2 fixation with various epoxides, and above 93% yields of the corresponding cyclic carbonates were detected at 80 °C, 0.1 MPa CO_2 pressure under solvent-free conditions. It could be predicted that the effectiveness of such a combination system originated from the synergetic interactions between π–π stacking, amino group and bromide ion nucleophile. This method provides a new strategy that the simple immobilized g-C_3N_4 can be used as a catalyst for the fixation reaction of CO_2 under mild conditions.

Author contributions

Tao Chang: Data curation, formal analysis, methodology, writing – original draft, review & editing. Xiaopeng Li: data curation, formal analysis. Yongjing Hao: data curation, formal analysis. Lianwei Kang: software, visualization. Tian Tian: data curation, methodology, software, supervision. Xiying Fu: data curation, software. Zheng Zhu: formal analysis, supervision. Balaji Panchal: writing – review & editing. Shenjun Qin: methodology, supervision, project administration, resources.

Conflicts of interest

There are no conflicts to declare.

Acknowledgements

This work was supported by the National Natural Science Foundation of China (NSFC) program (21902041), the National Science Foundation of Hebei province (B2019402020 B2020402002 E2021402017) and the Science and Technology Project of Hebei Education Department (ZD2019002, ZD2019055, QN2020165).

Notes and references

1 M. Mikkelsen, M. Jørgensen and F. C. Krebs, *Energy Environ. Sci.*, 2010, **3**, 43–81.
2 G. Singh, J. Lee, A. Karakoti, R. Bahadur, J. B. Yi, D. Y. Zhao, K. Albahily and A. Vinu, *Chem. Soc. Rev.*, 2020, **49**, 4360–4404.
3 A. Modak, P. Bhanja, S. Dutta, B. Chowdhury and A. Bhaumil, *Green Chem.*, 2020, **22**, 4002–4033.
4 P. Sreejyothi and K. M. Swadhin, *Chem. Sci.*, 2020, **11**, 10571–10593.
5 Z. E. Zhang, S. Y. Pan, H. Li, J. C. Cai, A. G. Olabi, E. J. Anthony and V. Manovic, *Renewable Sustainable Energy Rev.*, 2020, **125**, 109799.
6 M. Aresta, F. Nocito and A. Dibenedetto, *Adv. Catal.*, 2018, **62**, 49–111.
7 X. L. Liu, J. L. Li, N. Li, B. Y. Li and X. H. Bu, *Chin. J. Chem.*, 2021, **39**, 440–462.
8 C. Claver, M. B. Yeamin, M. Reguero and A. M. Masdeu-Bultó, *Green Chem.*, 2020, **22**, 7665–7706.
9 A. A. Marciniak, K. J. Lamb, L. P. Ozorio, C. J. A. Mota and M. North, *Curr. Opin. Green Sustain. Chem.*, 2020, **26**, 100365.
10 F. D. Monica and A. W. Kleij, *Catal. Sci. Technol.*, 2020, **10**, 3483–3501.
11 C. K. Ran, X. W. Chen, Y. Y. Gui, J. Liu, L. Song, K. Ren and D. G. Du, *Sci. China: Chem.*, 2020, **63**, 1336–1351.
12 B. Limburg, A. Cristofol, F. D. Monica and A. J. Kleij, *ChemSuschem*, 2020, **13**, 6056–6065.
13 S. L. Hou, J. Dong and B. Zhao, *Adv. Mater.*, 2019, **32**, 1806163.
14 F. D. Monica, A. Buonerba and C. Capacchione, *Adv. Synth. Catal.*, 2020, **361**, 265–282.
15 A. J. Kamphuis, F. Picchioni and P. P. Pescarmona, *Green Chem.*, 2019, **21**, 406–448.

16 K. Huang, J. Y. Zhang, F. J. Liu and S. Dai, *ACS Catal.*, 2018, **8**, 9079–9102.
17 B. Schäffer, F. Schäffner, S. P. Verevkin and A. Börner, *Chem. Rev.*, 2010, **110**, 4554–4581.
18 N. Yadav, F. Ssidi, D. Crespy and V. Dielia, *ChemSusChem*, 2019, **12**, 724–754.
19 J. H. Wu, B. H. Lv, X. M. Wu, Z. M. Zhou and G. Jing, *ACS Sustainable Chem. Eng.*, 2019, **7**, 7312–7323.
20 W. Sun, M. Wang, Y. Zhang, W. Ding, F. Huo, L. Wei and H. He, *Green Energy Environ.*, 2020, **5**, 183–194.
21 S. Suleman, H. A. Younus, Z. A. K. Khattak, H. Ullah, M. Elkadi and F. Verpoort, *Mol. Catal.*, 2020, **493**, 111071.
22 C. Sperandio, J. Rodriguez and A. Quintard, *Org. Biomol. Chem.*, 2020, **18**, 2637–2640.
23 K. Naveen, H. Ji, T. S. Kim, D. Kim and D. H. Cho, *Appl. Catal., B*, 2021, **280**, 119395.
24 Z. X. Yue, M. Pudukudy, S. Y. Chen, W. B. Zhao, J. Y. Wang, S. Y. Shan and Q. M. Jia, *Appl. Catal., A*, 2020, **601**, 117646.
25 J. Liu, G. Q. Yang, Y. Liu, D. J. Zhang, X. B. Hu and Z. B. Zhang, *Green Chem.*, 2020, **22**, 4509–4515.
26 X. Xin, H. W. Shan, T. Tian, Y. R. Wang, D. Yuan, H. P. You and Y. M. Yao, *ACS Sustainable Chem. Eng.*, 2020, **8**, 13185–13194.
27 Q. J. Wu, M. J. Mao, J. X. Chen, Y. B. Huang and R. Cao, *Catal. Sci. Technol.*, 2020, **10**, 8026–8033.
28 Y. Hao, T. Tian, Y. Kang, T. Chang, X. Fu, Z. Zhu, X. Meng, B. Panchala and S. Qin, *New J. Chem.*, 2020, **44**, 15811–15815.
29 H. Y. Cheng and T. Wang, *Adv. Synth. Catal.*, 2021, **363**, 144–193.
30 M. L. Ding, R. W. Flaig, H. L. Jiang and O. M. Yaghi, *Chem. Soc. Rev.*, 2019, **48**, 2783–2828.
31 Y. J. Hao, X. L. Yan, Z. Zhu, T. Chang, X. C. Meng, X. Y. Fu, B. Panchal, L. W. Kang and S. J. Qin, *Sustainable Energy Fuels*, 2021, **5**, 2943–2951.
32 T. Ema, K. Fukuhara, T. Sakai, M. Ohbo, F. Q. Bai and J. Y. Hasegawa, *Catal. Sci. Technol.*, 2015, **5**, 2314–2321.
33 J. P. Dong, C. Zhao, J. J. Qiu and C. M. Liu, *J. Ind. Eng. Chem.*, 2020, **90**, 95–104.
34 R. Yan, K. Chen, Z. J. Li, Y. Y. Qu, L. Y. Guo, H. Y. Tong, Y. Q. Li, J. Li, Y. Z. Hu and K. Guo, *ChemSusChem*, 2021, **14**, 738–744.
35 H. Q. Yang, D. N. Zheng, J. S. Zhang, K. Chen, J. F. Li, L. Wang, J. L. Zhang, H. Y. He and S. J. Zhang, *Chem. Ind. Eng. Prog.*, 2018, **57**, 7121–7129.
36 T. Chang, X. Gao, L. Bian, X. Fu, M. Yuan and H. Jing, *Chin. J. Catal.*, 2015, **36**, 408–413.
37 X. Fu, P. Xie, Y. Lian, L. He, W. Zhao, T. Chang and S. Qin, *Chin. J. Catal.*, 2018, **39**, 1854–1860.
38 M. Liu, X. Wang, Y. Jiang, J. Sun and M. Arai, *Catal. Rev.*, 2018, **61**, 214–267.
39 A. Thomas, A. Fischer, F. Goettmann, M. Antonietti, J.-O. Müller, R. Schlögl and J. M. Carlsson, *J. Mater. Chem.*, 2008, **18**, 4893–4908.
40 Z. J. Huang, F. B. Li, B. F. Chen, T. Lu, Y. Yuan and G. Q. Yuan, *Appl. Catal., A*, 2013, **136–137**, 269–277.
41 Q. Su, J. Sun, J. Q. Wang, Z. F. Yang, W. G. Cheng and S. J. Zhang, *Catal. Sci. Technol.*, 2014, **4**, 1556–1662.
42 J. Xu, F. Wu, Q. jiang, J. K. Shang and Y. X. Li, *J. Mol. Catal. A: Chem.*, 2015, **403**, 77–83.
43 J. Xu, J. K. Shang, Q. Jiang, Y. Wang and Y. X. Li, *RSC Adv.*, 2016, **6**, 55382–55392.
44 D. H. Lan, H. T. Wang, L. Chen, C. T. Au and S. F. Yin, *Carbon*, 2016, **100**, 81–89.
45 J. Xu, F. Wu, Q. Jiang and Y. X. Li, *Catal. Sci. Technol.*, 2015, **5**, 447–454.
46 Z. J. Huang, F. B. Li, B. F. Chen and G. Q. Yuan, *Catal. Sci. Technol.*, 2016, **6**, 2942–2948.
47 Y. Oh, V. D. Le, U. N. Maiti, J. O. Hwang, W. J. Park, J. Lim, K. E. Lee, Y. S. Bae, Y. H. Kim and S. O. Kim, *ACS Nano*, 2015, **9**, 9148–9157.
48 T. Biswas and V. Mahalingam, *New J. Chem.*, 2018, **41**, 14839–14842.
49 Y. Y. Yang, H. Li, S. P. Pei, F. Liu, W. Feng and Y. M. Zhang, *RSC Adv.*, 2020, **10**, 42408–42412.
50 H. Chand, P. Choudhary, A. Kumar, A. Kumar and V. Krishnan, *J. CO_2 Util.*, 2021, **51**, 101646.
51 J. Zhu, T. Diao, W. Wang, X. Xu, X. Sun, S. A. Carabineiro and Z. Zhao, *Appl. Catal., B*, 2017, **219**, 92–100.
52 X. H. Song, Y. F. Wu, D. H. Pan, F. F. Cai and G. M. Xiao, *Mol. Catal.*, 2017, **436**, 228–236.
53 S. Zhang, H. hang, F. X. Cao, Y. Y. Ma and Y. Q. Qu, *ACS Sustainable Chem. Eng.*, 2018, **6**, 4204–4211.
54 Y. Q. Gu, R. Ping, F. S. Liu, G. Y. Zhang, M. S. Liu and J. M. Sun, *Ind. Eng. Chem. Res.*, 2021, **60**, 5723–5732.
55 E. Peris, *Chem. Commun.*, 2016, **52**, 5777–5787.
56 M. Majdoub and Z. Anfar, *ACS Nano*, 2020, **14**, 12390–12469.
57 X. J. Zhang, B. Y. Wang, Y. M. Lu, C. G. Xia and J. H. Liu, *Mol. Catal.*, 2021, **504**, 111452.
58 X. Zhang, C. C. Jia, Y. H. Xue and P. Yang, *RSC Adv.*, 2017, **7**, 43888–43893.
59 J. Zhang, X. Li, Z. Zhu, T. Chang, X. Fu, Y. Hao, X. Meng, B. Panchal and S. Qin, *Adv. Sustainable Syst.*, 2021, **5**, 2000133.
60 X. Jiang, F. L. Gou, F. Chen and H. W. Jing, *Green Chem.*, 2016, **18**, 3567–3576.
61 J. Y. Wang, Y. T. Liang, D. G. Zhou, J. P. Ma and H. W. Jing, *Org. Chem. Front.*, 2018, **5**, 741–748.
62 Y. D. Zhang, G. J. Chen, L. Wu, K. Liu, H. Zhong, Z. Y. Long, M. M. Tong, Z. Z. Yang and S. Dai, *Chem. Commun.*, 2020, **56**, 3309–3312.
63 K. Pramoda, U. Gupta, M. Chhetri, A. Bandyopadhyay, S. K. Pati and C. N. R. Rao, *ACS Appl. Mater. Interfaces*, 2017, **9**, 10664–10672.
64 F. L. Lai, Y. Wang, D. D. Li, X. S. Sun, J. Peng, X. D. Zhang, Y. P. Tian and T. X. Liu, *Nano Res.*, 2018, **11**, 1099–1108.
65 X. C. Wang, K. Maeda, A. Thomas, K. Takanabe, G. Xin, J. M. Carlsson, K. Domen and M. Antonietti, *Nat. Mater.*, 2009, **8**, 76–80.